Electronic properties of $Sc_5M_4Si_{10}$ (M=Co,Rh,Ir) probed by NMR and first-principles calculations

C. S. Lue,* R. F. Liu,† Y. F. Fu, and C. Cheng
Department of Physics, National Cheng Kung University, Tainan 70101, Taiwan

H. D. Yang
Department of Physics, National Sun Yat-Sen University, Kaohsiung 80424, Taiwan

(Received 14 November 2007; revised manuscript received 3 January 2008; published 21 March 2008)

We report a systematic study of ^{45}Sc NMR measurements on the $Sc_5Co_4Si_{10}$-type silicides $Sc_5M_4Si_{10}$ (M=Co,Rh,Ir). From the central transition line shapes, three nonequivalent Sc sites have been identified. We thus measured the Knight shift and spin-lattice relaxation time (T_1) for each of the three crystallographic sites. Results of experimental Knight shift and T_1 together with theoretical band structure calculations provide evidence that orbital electrons are responsible for the observed shifts as well as the relaxation rates. In addition, we found no correlation between the Fermi-level density of states and the superconducting transition temperature of the studied materials. Further analyses clearly indicate that the effect of electron-phonon coupling plays a significant role for the superconductivity of $Sc_5M_4Si_{10}$, and these materials should be classified as moderate-coupling superconductors.

DOI: 10.1103/PhysRevB.77.115130 PACS number(s): 76.60.−k, 71.20.−b, 71.20.Be

I. INTRODUCTION

Ternary silicide $Sc_5Co_4Si_{10}$ exhibits superconducting behavior (transition temperature T_c=4.9 K) in spite of the presence of a significant amount of magnetic 3d element.[1,2] The isostructural compounds $Sc_5Rh_4Si_{10}$ and $Sc_5Ir_4Si_{10}$ are also superconductors with relatively high transition temperatures of 8.4 and 8.6 K, respectively.[3] It has been speculated that the superconductivity of this system is attributed to the large density of states (DOS) at the Fermi level, especially for $Sc_5Rh_4Si_{10}$ and $Sc_5Ir_4Si_{10}$. Contrary to the expectation, the low-temperature specific heat coefficient (γ) measurement, which is usually connected to the normal electronic Fermi-level DOS, indicated the largest γ value in $Sc_5Co_4Si_{10}$ among the silicides of this prototype.[4] However, the extracted γ for $Sc_5Rh_4Si_{10}$ and $Sc_5Ir_4Si_{10}$ have been argued to be unreliable because their higher T_c might render the extrapolation of the fit below T_c less accurate. Nevertheless, there has been no other experimental work associated with these scenarios, essential to interpret their electronic properties.

The crystal structure of $Sc_5M_4Si_{10}$ is primitive tetragonal (space group $P4/mbm$) and contains 38 atoms per unit cell, as illustrated in Fig. 1. Within this structure, M and Si atoms stack along the c axis via M-Si-M zigzag chains, separated by layers of Sc atoms.[5] There are three nonequivalent Sc sites denoted as Sc-I, Sc-II, and Sc-III with population ratio of 1:2:2. The Sc-I site has the highest local symmetry along the c axis, while the Sc-II and Sc-III atoms are embedded within pentagonal and hexagonal layers, respectively. It is interesting to note that there is an absence of direct M-M metal contacts in this structure. The M atoms are linked to each other through Sc and Si elements. Therefore, the interactions between M and Sc atoms would play important roles for their electronic band features. With the study of interactions between different M atoms and individual Sc sites, the results can be utilized to examine the local electronic properties of $Sc_5M_4Si_{10}$. Nuclear magnetic resonance (NMR) is known as an atomic probe in metallic alloys yielding information on site occupation and Fermi surface features.[6] In this paper, we will present ^{45}Sc NMR measurements including the Knight shifts as well as spin-lattice relaxation times in $Sc_5Co_4Si_{10}$, $Sc_5Rh_4Si_{10}$, and $Sc_5Ir_4Si_{10}$ as related to their electronic characteristics and superconductivity. In a parallel study, *ab initio* calculations were also performed to obtain the electronic DOS for comparison.

II. RESULTS AND DISCUSSION

Polycrystalline samples were prepared by arc melting stoichiometric amounts of the elements in a Zr-gettered argon atmosphere. Each material was melted several times, and the weight loss during melting was negligible. To promote homogeneity, all studied compounds were annealed in

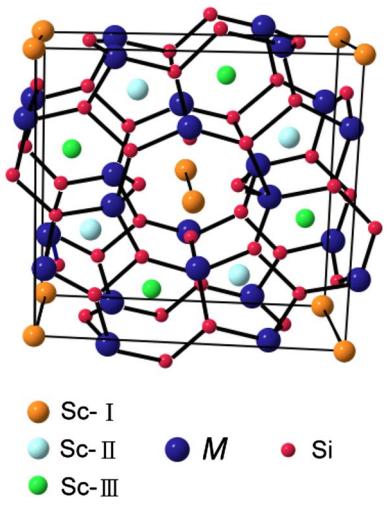

FIG. 1. (Color online) Crystal structure for $Sc_5M_4Si_{10}$.

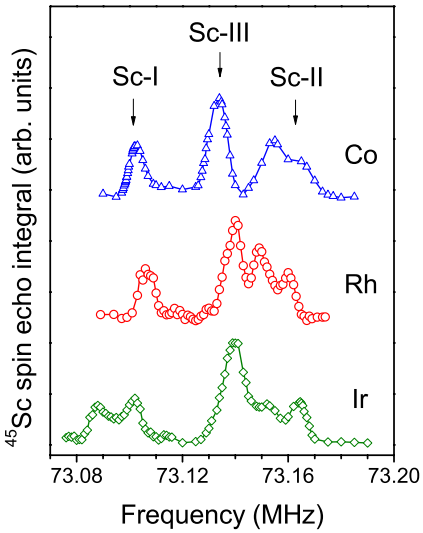

FIG. 2. (Color online) Resolved ^{45}Sc central transition NMR spectra for $Sc_5M_4Si_{10}$ (M=Co,Rh,Ir) measured at room temperature.

a sealed quartz tube under 150 Torr of argon at 1050 °C for 18 days, followed by a water quench to room temperature. Powder x-ray diffraction data confirmed the single phase with the expected $Sc_5Co_4Si_{10}$-type structure.

NMR measurements were performed in a constant field of 7.0665 T. A home-built probe was employed for both room-temperature and low-temperature experiments.[7] Since the studied materials are metals, powder samples were used to avoid the skin depth problem of the rf transmission power. Each specimen was set in a plastic vial that showed no observable ^{45}Sc NMR signal. The Knight shifts here were referred to the ^{45}Sc resonance frequency of aqueous $ScCl_3$.

A. Line shapes and Knight shifts

Room-temperature ^{45}Sc NMR central transition ($m=\frac{1}{2}\leftrightarrow-\frac{1}{2}$) line shapes for $Sc_5Co_4Si_{10}$, $Sc_5Rh_4Si_{10}$, and $Sc_5Ir_4Si_{10}$ were displayed in Fig. 2, obtained by integrating spin echo signals of various excitations. For each individual material, three distinctive Sc sites are well resolved. Since the population of Sc-I is one-half of that of other scandium sites, the low-frequency peak with a smaller line shape area should be assigned to this site. For Sc-II atoms, they are located inside pentagons which have a lower symmetry in the crystallographic environment, resulting in a wider quadrupolar broadening in the central transition line. With this accordance, the high-frequency part which splits into two peaks is associated with Sc-II. The remaining line which appears at the center of the spectrum is thus attributed to Sc-III.

It is remarked that the feature of line shapes remains unchanged with temperature, signifying nonmagnetic nature for these materials at normal states. This finding is particularly important for $Sc_5Co_4Si_{10}$ because this compound contains a substantial amount of Co element. Thus, the NMR observation confirms the absence of magnetic moment on the Co site of $Sc_5Co_4Si_{10}$.

TABLE I. Isotropic Knight shift (10^{-3}%) and experimental, d-electron, and orbital electron $1/T_1T$ values (10^{-3} s^{-1} K^{-1}) for each of the Sc sites.

Alloy	Site	K_{iso}	$(1/T_1T)_{expt}$	$(1/T_1T)_d$	$(1/T_1T)_{orb}$
$Sc_5Co_4Si_{10}$	I	2.5 ± 0.3	10.6	1.3	9.3
	II	10.4 ± 0.8	8.4	3.9	4.5
	III	6.7 ± 0.4	14.7	4.6	10.1
$Sc_5Rh_4Si_{10}$	I	3.3 ± 0.3	15.4	1.1	14.3
	II	10.1 ± 0.9	10.4	4.2	6.2
	III	7.8 ± 0.5	20.9	5.5	15.4
$Sc_5Ir_4Si_{10}$	I	2.2 ± 0.4	16.1	0.7	15.4
	II	10.3 ± 0.9	14.7	3.6	11.1
	III	7.5 ± 0.4	20.1	3.8	16.3

For each individual Sc site, the isotropic Knight shift (K_{iso}) was estimated from the center of the gravity of the corresponding transition line with results summarized in Table I. Universally small K_{iso} values ranging from 10^{-3}% to 10^{-2}% were extracted for all of the three Sc sites in $Sc_5M_4Si_{10}$. This observation is consistent with a previous NMR study of $Sc_5Ir_4Si_{10}$ which also showed a tiny positive ^{45}Sc Knight shift although the shift was an averaged result of three Sc sites.[8] For ordinary d-electron metals, K_{iso} can be expressed as $K_{iso}=K_{orb}+K_d$. Here, K_{orb} represents the orbital Knight shift, arising from the orbital magnetic moment of electrons induced by the applied field. K_d is the d-spin shift which involves the spin polarization of the closed s shells and of the s-character electrons in the conduction bands via d electrons. Note that K_d is negative due to the antiparallel orientation between core spins and the unpaired spins responsible for the polarization.[9] For all studied materials, the determined K_{iso} values are positive, indicative of a minor contribution from d electrons on the frequency shift. While the s-contact Knight shift is usually comparable with K_d in d-electron based materials, we omitted this term because of the extremely low Fermi-level s-DOS for the present compounds. Indeed, the calculated partial Fermi-level DOS (see Table II) confirms that Sc Fermi-level d-DOS is considerably larger than s-DOS for these compounds. With this respect, an observation of the small positive values of K_{iso} implies that the isotropic Knight shifts in all Sc sites are mainly due to orbital electrons.

B. Spin-lattice relaxation rates

The spin-lattice relaxation time (T_1) measurements were carried out using the inversion recovery method. We recorded the signal strength by integrating the recovered spin echo signal. Since the central transition spectrum shows distinctive peaks for the corresponding Sc site, we found each T_1 by centering the transmission frequency at each individual line, where the resonance is dominated by one site. In these experiments, the relaxation process involves the adjacent pairs of spin levels, and the corresponding spin-lattice relaxation is a multiexponential expression.[10] For the central tran-

TABLE II. Calculated Sc partial Fermi-level *s*-, *p*-, *d*-, and total DOSs (states/eV atom) for each individual crystallographic site.

Alloy	Site	*s*	*p*	*d*	Total
$Sc_5Co_4Si_{10}$	I	0.0099	0.025	0.454	0.4893
	II	0.0141	0.052	0.798	0.8644
	III	0.0106	0.026	0.866	0.9027
$Sc_5Rh_4Si_{10}$	I	0.0146	0.032	0.419	0.4653
	II	0.0146	0.053	0.824	0.8905
	III	0.0132	0.030	0.942	0.9849
$Sc_5Ir_4Si_{10}$	I	0.0085	0.033	0.338	0.3789
	II	0.0128	0.048	0.767	0.8273
	III	0.0114	0.037	0.781	0.8282

sition with $I=\frac{7}{2}$, the recovery of the nuclear magnetization is as follows:

$$\frac{M(t)-M(\infty)}{M(\infty)} = -2\alpha(0.012e^{-t/T_1}+0.068e^{-6t/T_1} + 0.206e^{-15t/T_1}+0.714e^{-28t/T_1}), \quad (1)$$

derived from the initial conditions used in our experiments. Here, $M(t)$ is the magnetization at the recovery time t and $M(\infty)$ is the magnetization after long time recovery. The parameter α is a fractional value derived from the initial conditions used in our experiments. Each experimental T_1 was thus obtained by fitting to this multiexponential recovery curve. Note that the Korringa behavior (constant T_1T) (Ref. 11) was found for measurements between 77 and 295 K, confirming a conduction electron mechanism for the observed relaxation.

As in the case of the Knight shift, two relaxation mechanisms may dominate the experimental ^{45}Sc T_1: $(1/T_1)_{expt}=(1/T_1)_d+(1/T_1)_{orb}$. The first term arises from the *d*-spin core polarization, while the last one is due to orbital electrons. Since the NMR relaxation rate is weakly enhanced by electron-electron interactions in a nonmagnetic metal, $(1/T_1)_d$ can be considered to measure the band density of states. Based on the noninteracting electron picture, $(1/T_1T)_d$ can be expressed as

$$\left(\frac{1}{T_1T}\right)_d = 2hk_B[\gamma_n H_{hf}^d N_d(E_F)]^2 q. \quad (2)$$

Here h, k_B, and γ_n are the Planck constant, the Boltzmann constant, and the Sc nuclear gyromagnetic ratio. H_{hf}^d is the hyperfine field per electron of the Sc *d* electrons and $N_d(E_F)$ is the partial Fermi-level *d*-DOS in units of states/eV spin. The parameter q is a reduction factor which depends on the relative weight at the Fermi-level of the irreducible representations of the atomic *d* functions.

For each Sc site in $Sc_5M_4Si_{10}$, the values of $N_d(E_F)$ have been revealed from the first-principles electronic structure calculations, as will be presented later. Taking $H_{hf}^d \sim -6.4\times10^4$ g in Sc metals and $q=0.2$ for the case of an equal contribution from all five orbitals,[12] the values of $(1/T_1T)_d$ ranging from $(1-5)\times10^{-3}$ s^{-1} K^{-1} for all probed Sc sites were deduced. The orbital part can be thus isolated by means of $(1/T_1T)_{orb}=(1/T_1T)_{expt}-(1/T_1T)_d$ with the results tabulated in Table I. It is found that $(1/T_1T)_{orb}$ is greater than $(1/T_1T)_d$ for each Sc site of $Sc_5M_4Si_{10}$, indicating that orbital electrons play a key role for the observed relaxations. Such a result is consistent with the Knight shift showing orbital electrons responsible for the observed shifts.

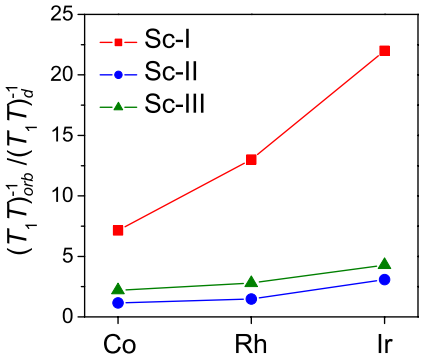

FIG. 3. (Color online) Ratio of $(\frac{1}{T_1T})_{orb}/(\frac{1}{T_1T})_d$ for each Sc site of $Sc_5M_4Si_{10}$ (M=Co, Rh, Ir).

As analogous to $(1/T_1T)_d$, the orbital term can be written as

$$\left(\frac{1}{T_1T}\right)_{orb} = 2hk_B[\gamma_n H_{hf}^{orb} N_d(E_F)]^2 p, \quad (3)$$

where H_{hf}^{orb} is the orbital hyperfine field per unit orbital angular momentum and $p=0.4$ is the reduced factor for the equal orbital weight at the Fermi surface. Hence, the combination of Eqs. (2) and (3) gives the ratio of $(\frac{1}{T_1T})_{orb}/(\frac{1}{T_1T})_d = 2(H_{hf}^{orb}/H_{hf}^d)^2$ which provides a measure of H_{hf}^{orb} for each individual Sc site of the corresponding compound. From the relation of $H_{hf}^{orb}=\gamma_e\hbar\langle r^{-3}\rangle$, where $\langle r^{-3}\rangle$ represents an average over the radial distribution of the scandium *d* electrons at the Fermi surface, one can find the tendency of $\langle r^{-3}\rangle$ directly from $(\frac{1}{T_1T})_{orb}/(\frac{1}{T_1T})_d$ of $Sc_5M_4Si_{10}$. It is remarked that for each Sc site, the value of $(\frac{1}{T_1T})_{orb}/(\frac{1}{T_1T})_d$ increases when going from $Sc_5Co_4Si_{10}$ to $Sc_5Ir_4Si_{10}$, as illustrated in Fig. 3. This clearly demonstrates a reducing trend in $\langle r^{-3}\rangle$ which means that more electrons involve in chemical bonding and get localized. Accordingly, lower Sc partial Fermi-level DOSs are expected in $Sc_5Rh_4Si_{10}$ and $Sc_5Ir_4Si_{10}$, which agree well with the calculated results, as will be addressed in the next section.

Another interesting trend revealed from Fig. 3 is a relative large value of $(\frac{1}{T_1T})_{orb}/(\frac{1}{T_1T})_d$ which consistently appears in Sc-I. This means a smaller $\langle r^{-3}\rangle$, more localized *d* orbitals, at this site. Such a characteristic is particularly pronounced in the isostructural compounds $Lu_5Ir_4Si_{10}$ and $Lu_5Rh_4Si_{10}$, which exhibit the coexistence of superconductivity and charge-density-wave (CDW) transitions.[13,14] The presence of CDW behavior in both Lu-based silicides has been attributed to the formation of quasi-one-dimensional chains along Lu-I atoms,[15] equivalent to the Sc-I site in $Sc_5M_4Si_{10}$. With this

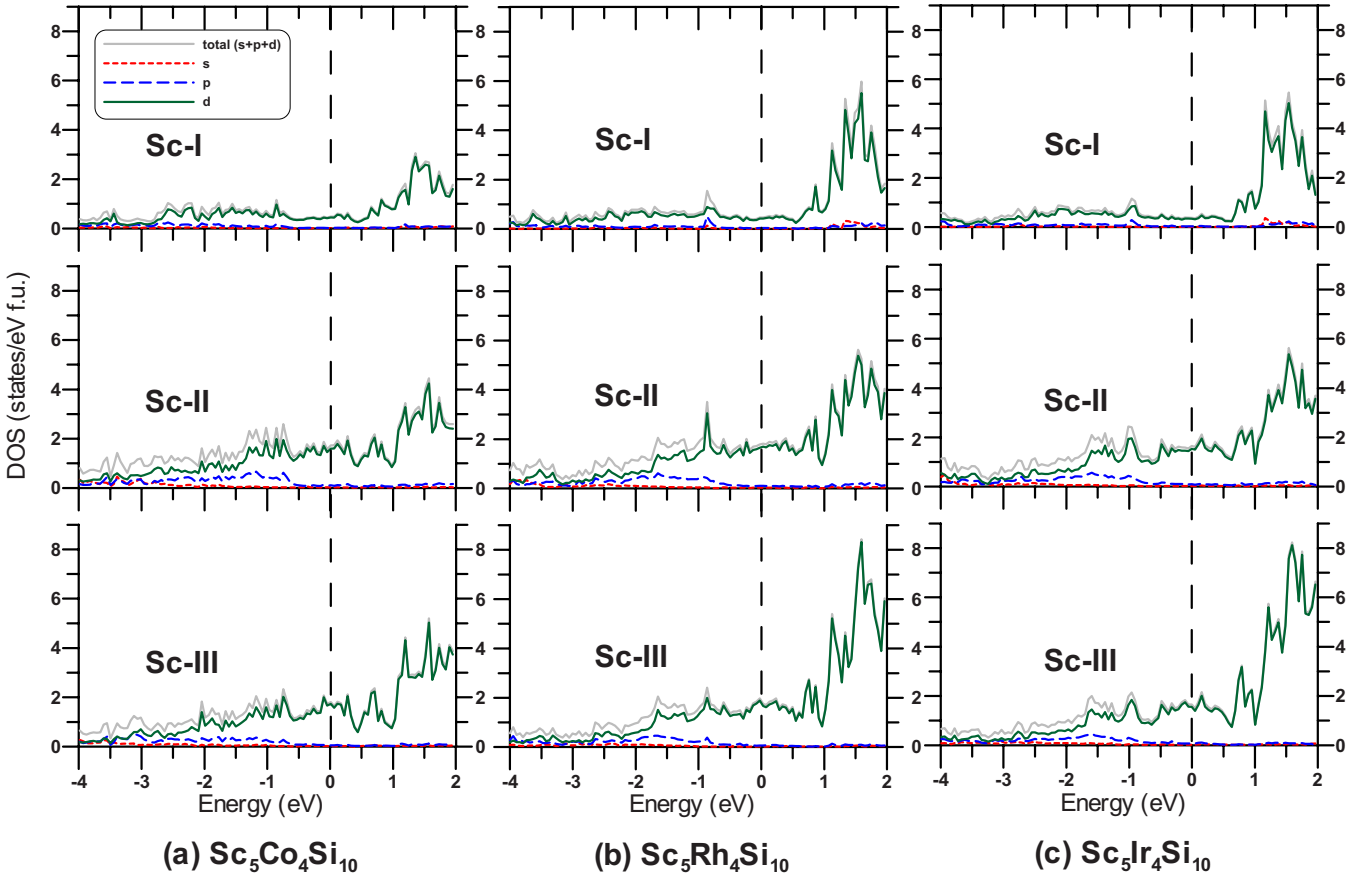

FIG. 4. (Color online) Site-decomposed density of states for $Sc_5Co_4Si_{10}$, $Sc_5Rh_4Si_{10}$, and $Sc_5Ir_4Si_{10}$. The zero of the energy denotes the Fermi level of the corresponding material.

comparison, we consider that the site-I atom with rather localized *d* orbitals is a common feature among the $Sc_5Co_4Si_{10}$-type silicides.

C. First-principles calculations

Theoretical results from first-principles calculations are presented in this section. We have calculated the total DOSs of $Sc_5M_4Si_{10}$ (M=Co, Rh, Ir), orbital-projected partial DOSs for three Sc sites, and the partial DOSs for different M elements. Our calculations are based on the density functional theory.[16] The generalized gradient approximation by Perdew and Wang was used to represent the exchange-correlation energy functional in the systems.[17,18] The interaction between core and valence electrons was described by projector augmented-wave method[19] implemented by Kresse and Joubert.[20] There are three and four valence electrons included in the calculations for Sc and Si atoms, respectively, and nine valance electrons for Co, Ir, and Rh atoms. The one-electron Kohn-Sham wave functions were expanded by plane-wave basis with kinetic energy cutoff of 307 eV. We sampled k points in the Brillouin zone by using Monkhorst-Pack technique.[21] K-point grids of (8 8 24) are sufficient for the present systems. Self-consistency was achieved when the total energy change and the band structure energy change between two iterations were both smaller than 10^{-4} eV. All calculations here were performed by using Vienna *ab initio* simulation package (VASP).[22,23]

The structures for these compounds were fully relaxed such that the atomic forces in the unit cell are smaller than 0.02 eV/Å. The calculated lattice constants are a=12.01 Å and c=3.933 Å for $Sc_5Co_4Si_{10}$, a=12.389 Å and c=4.051 Å for $Sc_5Rh_4Si_{10}$, and a=12.397 Å and c=4.089 Å for $Sc_5Ir_4Si_{10}$. These results compare well with the experimental values for the corresponding compound.[3]

The orbital-projected partial DOSs for three different Sc sites of individual materials are illustrated in Fig. 4. The obtained partial Fermi level DOSs for the *s*, *p*, and *d* electrons of scandium atoms are given in Table II. It is apparent that the contributions of Sc atoms at the Fermi level are mostly from *d* electrons. The results of $N_d(E_F)$ for individual Sc sites have been used to calculate $(1/T_1T)_d$ which appear to be reasonable as compared to the experimental values.

In Fig. 5, we present the calculated total as well as the atom-decomposed density of states for $Sc_5Co_4Si_{10}$, $Sc_5Rh_4Si_{10}$, and $Sc_5Ir_4Si_{10}$. The partial Fermi-level DOSs arising from Sc, M (Co, Rh, Ir), and Si atoms are summarized in Table III. It shows that the DOS at the Fermi level is dominated by the states of Sc and M atoms, which contribute about 83–86% of the total DOS. However, a marked difference in comparison to $Sc_5Co_4Si_{10}$ is the decreasing contribution of Rh 4*d* and Ir 5*d* states to the Fermi-level DOS; in $Sc_5Co_4Si_{10}$, the Fermi-level DOS is shared almost equally by the Sc and Co 3*d* states. The reduction of Fermi-level DOSs

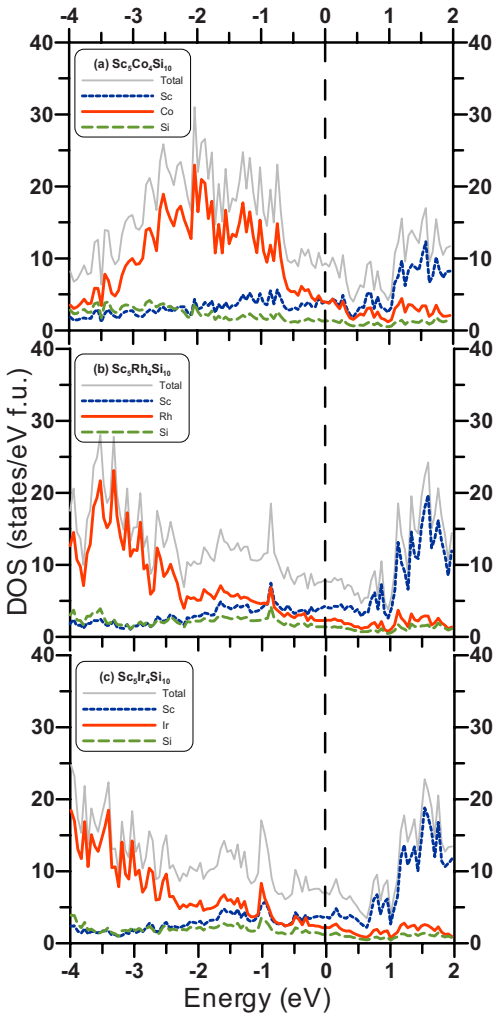

FIG. 5. (Color online) Total and projected density of states for $Sc_5Co_4Si_{10}$, $Sc_5Rh_4Si_{10}$, as well as $Sc_5Ir_4Si_{10}$. Each Fermi level is at zero energy indicated by a dashed line.

in $Sc_5Rh_4Si_{10}$ and $Sc_5Ir_4Si_{10}$ can be related to their higher phase stability. This can be understood as follows: If the Fermi-level DOS is small, it means that more electrons participate in bonding and thus get localized. As a result, the stability of the material will be larger. With this accordance, the present study implies that $Sc_5Rh_4Si_{10}$ and $Sc_5Ir_4Si_{10}$ are more stable than $Sc_5Co_4Si_{10}$ with respect to the $Sc_5Co_4Si_{10}$-type structure. In addition, for the isoelectronic compounds, the one with lower Fermi-level DOS will reflect itself to a smaller bulk modulus. On this basis, a larger bulk modulus in $Sc_5Co_4Si_{10}$ is thus expected.

From the calculated total Fermi-level density of states $N(E_F)$, the electron-phonon coupling constant λ_{ep} can be estimated using the values of γ and $N(E_F)$ according to the relation

$$\gamma = \frac{\pi^2 k_B^2}{6} N(E_F)[1 + \lambda_{ep}]. \quad (4)$$

We found $\lambda_{ep}=0.43$ for $Sc_5Co_4Si_{10}$, quite close to the value of 0.47 obtained from the analysis of low-temperature specific heat data.[4] However, unreasonably negative values were yielded for $Sc_5Rh_4Si_{10}$ and $Sc_5Ir_4Si_{10}$, suggesting that the reported γ values for both materials should be underestimated. We now estimate the Coulomb coupling constant μ^* using McMillian's formula[24,25] as

$$T_c = \frac{\theta_D}{1.45} \exp\left[-\frac{1.04(1 + \lambda_{ep})}{\lambda_{ep} - \mu^*(1 + 0.62\lambda_{ep})} \right]. \quad (5)$$

Taking the Debye temperature $\theta_D=548$ K,[4] $T_c=4.89$ K, and $\lambda_{ep}=0.43$ for $Sc_5Co_4Si_{10}$, $\mu^*=0.073$ was thus determined. Assuming this value is valid for $Sc_5Rh_4Si_{10}$ and $Sc_5Ir_4Si_{10}$, one can extract each λ_{ep} by means of

$$\lambda_{ep} = \frac{1.04 + \mu^* \ln\left(\frac{\theta_D}{1.45T_c}\right)}{(1 - 0.62\mu^*)\ln\left(\frac{\theta_D}{1.45T_c}\right) - 1.04}. \quad (6)$$

With reported $\theta_D=448$ and 402 K, and $T_c=8.43$ and 8.57 K for $Sc_5Rh_4Si_{10}$ and $Sc_5Ir_4Si_{10}$, respectively,[4] we thus found $\lambda_{ep}=0.54$ for $Sc_5Rh_4Si_{10}$ and $\lambda_{ep}=0.57$ for $Sc_5Ir_4Si_{10}$. Both values suggest that $Sc_5Rh_4Si_{10}$ and $Sc_5Ir_4Si_{10}$ are moderate-coupling superconductors.

As mentioned, the experimental γ values of $Sc_5Rh_4Si_{10}$ and $Sc_5Ir_4Si_{10}$ should be inaccurate because their higher T_c render the extrapolation of the fit below T_c unreliable. Here, we estimate γ from Eq. (4) with reasonable $N(E_F)$ and λ_{ep}. Reliable values of $\gamma=28.7$ and 26.3 mJ/mol K^2 for $Sc_5Rh_4Si_{10}$ and $Sc_5Ir_4Si_{10}$, respectively, were thus obtained. These two values are much larger than the reported ones,[4] and the measurement of low-temperature specific heat under magnetic field which could suppress the superconducting transition would help with the verification. Taking the specific heat jump $\Delta C=252$ mJ/mol K in $Sc_5Ir_4Si_{10}$,[4] it yields $\Delta C/\gamma T_c=1.12$, a bit less than 1.43 expected from BCS theory. Such a result is contrary to the previous conclusion, showing that $Sc_5Ir_4Si_{10}$ is a strong-coupled superconductor based on the large $\Delta C/\gamma T_c=2.96$ associated with a small $\gamma=9.93$ mJ/mol K^2.[4]

TABLE III. Calculated projected and total Fermi-level density of states (states/eV f.u.) for $Sc_5M_4Si_{10}$.

Alloy	Sc	M	Si	Total
M=Co	4.024	3.944	1.366	9.334
M=Rh	4.216	2.280	1.376	7.871
M=Ir	3.690	2.187	1.209	7.086

III. CONCLUSIONS

NMR measurements and first-principles calculations have provided a concise picture for the local electronic properties in $Sc_5Co_4Si_{10}$, $Sc_5Rh_4Si_{10}$, and $Sc_5Ir_4Si_{10}$. Important aspects established from this study are summarized as follows. (1) Orbital electrons are responsible for the observed Knight shifts as well as the spin-lattice relaxation rates in all Sc sites. (2) Clear evidence for the rather localized d orbitals in Sc-I was found, which is considered as a common feature among the $Sc_5Co_4Si_{10}$-type silicides. (3) $Sc_5Co_4Si_{10}$ pos-

sesses the largest Fermi-level DOS, as compared to $Sc_5Rh_4Si_{10}$ and $Sc_5Ir_4Si_{10}$. This implies that higher T_c in $Sc_5Rh_4Si_{10}$ and $Sc_5Ir_4Si_{10}$ are of no relevance with their electronic DOSs. Instead, T_c and λ_{ep} correlate well with each other, pointing that the electron-phonon coupling plays a significant role for the superconductivity of $Sc_5M_4Si_{10}$. (4) Analyses using the proposed γ values of $Sc_5Rh_4Si_{10}$ and $Sc_5Ir_4Si_{10}$ indicate that both materials should be classified as moderate-coupling superconductors, in contrast with the previous conclusion.

ACKNOWLEDGMENTS

We are grateful for the support from the National Science Council of Taiwan under Grant Nos. NSC-95-2112-M-006-021-MY3 (C.S.L) and NSC-96-2112-M-110-001 (H.D.Y).

*cslue@mail.ncku.edu.tw
†fmliu@phys.ncku.edu.tw

[1] H. F. Braun and C. U. Segre, Solid State Commun. **35**, 735 (1980).
[2] H. F. Braun and C. U. Segre, in *Ternary Superconductors*, edited by G. K. Shenoy, B. D. Dunlap, and F. Y. Fradin (North-Holland, New York, 1981), p. 239.
[3] H. D. Yang, R. N. Shelton, and H. F. Braun, Phys. Rev. B **33**, 5062 (1986).
[4] L. S. Hausermann-Berg and R. N. Shelton, Phys. Rev. B **35**, 6659 (1987).
[5] H. F. Braun, K. Yvon, and R. H. Braun, Acta Crystallogr., Sect. B: Struct. Crystallogr. Cryst. Chem. **36**, 2397 (1980).
[6] C. S. Lue, B. X. Xie, S. N. Horng, J. H. Su, and Y. J. Lin, Phys. Rev. B **71**, 195104 (2005).
[7] C. S. Lue, C. N. Kuo, T. H. Su, and G. J. Redhammer, Phys. Rev. B **75**, 014426 (2007).
[8] Po-Jen Chu, B. C. Gerstein, H. D. Yang, and R. N. Shelton, Phys. Rev. B **37**, 1796 (1988).
[9] *Metallic Shifts in NMR*, edited by G. C. Carter, L. H. Bennett, and D. J. Kahan (Pergamon, Oxford, 1977).
[10] A. Narath, Phys. Rev. **162**, 320 (1967).
[11] J. Korringa, Physica (Amsterdam) **16**, 601 (1950).
[12] B. Perrin, P. Descouts, A. Dupanloup, and D. Seipler, J. Phys. F: Met. Phys. **9**, 673 (1979).
[13] R. N. Shelton, L. S. Hausermann-Berg, P. Klavins, H. D. Yang, M. S. Anderson, and C. A. Swenson, Phys. Rev. B **34**, 4590 (1986).
[14] Y.-K. Kuo, C. S. Lue, F. H. Hsu, H. H. Li, and H. D. Yang, Phys. Rev. B **64**, 125124 (2001).
[15] B. Becker, N. G. Patil, S. Ramakrishnan, A. A. Menovsky, G. J. Nieuwenhuys, J. A. Mydosh, M. Kohgi, and K. Iwasa, Phys. Rev. B **59**, 7266 (1999).
[16] P. Hohenberg and W. Kohn, Phys. Rev. **136**, B864 (1964); W. Kohn and L. J. Sham, *ibid.* **140**, A1133 (1965).
[17] J. P. Perdew, in *Electronic Structure of Solids '91*, edited by P. Ziesche and H. Eschrig (Akademie-Verlag, Berlin, 1991).
[18] J. P. Perdew, J. A. Chevary, S. H. Vosko, K. A. Jackson, M. R. Pederson, D. J. Singh, and C. Fiolhais, Phys. Rev. B **46**, 6671 (1992).
[19] P. E. Blöchl, Phys. Rev. B **50**, 17953 (1994).
[20] G. Kresse and D. Joubert, Phys. Rev. B **59**, 1758 (1999).
[21] H. J. Monkhorst and J. D. Pack, Phys. Rev. B **13**, 5188 (1976).
[22] G. Kresse and J. Hafner, Phys. Rev. B **47**, 558 (1993); **49**, 14251 (1994).
[23] G. Kresse and J. Furthmuller, Comput. Mater. Sci. **6**, 15 (1996); Phys. Rev. B **54**, 11169 (1996).
[24] W. L. McMillan, Phys. Rev. **167**, 331 (1968).
[25] P. B. Allen and R. C. Dynes, Phys. Rev. B **12**, 905 (1975).